A 532 nm Chaotic Lidar Transmitter for High Resolution Underwater Ranging and Imaging

Luke K. Rumbaugh[1], Erik M. Bollt[2],
and William D. Jemison[1]
Department of [1]Electrical and Computer Engineering, [2]Mathematics
Clarkson University, Potsdam, New York 13676-5720
Email: rumbaulk@clarkson.edu

Yifei Li
Department of Electrical and Computer Engineering
University of Massachusetts Dartmouth
Dartmouth, Massachusetts

***Abstract*—A chaotic lidar transmitter based on an ultralong cavity fiber laser is presented for underwater ranging and imaging applications. Experimental results show 150 mW continuous output power at 532 nm, with wideband (>3 GHz) chaotic intensity modulation. An incoherent digital receiver is used to show a ranging accuracy of 1 cm in a water tank with a measurement-limited range resolution of ±4 cm. There is no range ambiguity because of the non-repeating nature of the chaotic signal.**

I. Introduction

Light detection and ranging (LIDAR) systems can be used for high-resolution ranging and high contrast imaging underwater [1]. The underwater channel presents lidar with unique challenges, especially in the absorption and scattering of light by water and particles [2]. Absorption of light by water can be minimized by using blue wavelengths in the open ocean or green wavelengths in coastal waters [3]. At these wavelengths, high power transmitters can operate at long standoff distances in absorption-limited environments. When operating in scattering-limited environments, however, increased power alone will not improve system performance: scattered light must be separated from the target signal.

Hybrid lidar-radar (HLR) is one technique that has been successfully used to improve system performance in scattering-limited scenarios [4]–[10]. HLR uses high frequency intensity modulation of the optical carrier to filter out the backscatter, since the backscatter's modulation starts to decorrelate at modulation frequencies above ∼100 MHz [11], [12]. Chaotic lidar is another technique that has the potential to improve system performance in scattering-limited scenarios. Chaotic lidar uses internally modulated chaotic lasers to generate non-repeating, wide bandwidth signals (>1 GHz), and has been successfully used in radar, lidar, and OTDR [13]–[15]. The chaotic waveform can support high resolution ranging with no range ambiguity. Further, chaotic lidar has the potential for excellent backscatter suppression in turbid water environments because of its inherent high frequency intensity modulation. To the best of our knowledge, chaotic lidar has never been implemented underwater.

In this paper, we introduce a 532 nm chaotic lidar transmitter designed for underwater ranging and imaging experiments. The transmitter uses an ultralong cavity fiber laser to generate the high frequency modulation required for scattering suppression [16]. The fiber laser produces the non-repeating wideband signal with no external modulator or RF source, and is scalable to high powers. The chaotic signal generated supports high resolution, unambiguous ranging, and will allow exploration of backscatter suppression at modulation frequencies that have yet to be explored experimentally. This transmitter is used with an incoherent digital noise radar receiver [17] to perform a ranging demonstration in a water tank, achieving 1 cm downrange accuracy and measurement-limited ±4 cm resolution, with no range ambiguity.

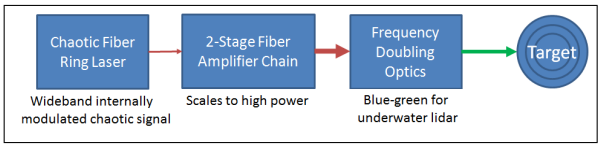

Fig. 1. Chaotic lidar transmitter for underwater ranging and imaging.

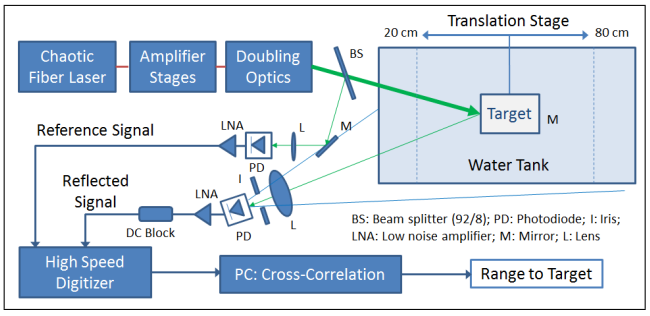

Fig. 2. Ranging demonstration using the 532 nm chaotic lidar transmitter.

In Section II we outline the design considerations for underwater lidar systems, and detail the design of our transmitter in response to these factors. Section III shows the construction and characterization of the transmitter, and Section IV presents the experimental results of our ranging demonstration. Section V draws conclusions and outlines future work.

II. Chaotic Lidar Transmitter Design

Figure 1 shows the 532 nm chaotic lidar transmitter. The transmitter consists of an internally modulated chaotic ytterbium-doped fiber ring laser (CYDFL), two fiber amplification stages, and a frequency doubler. The CYDFL is used to

generate a 1064 nm chaotic seed signal. Thousands of cavity modes lase simultaneously in this laser, generating a wide bandwidth modulation signal from DC to many GHz [18]. The wide bandwidth of the chaotic signal supports centimeter-resolution ranging, while the high frequency content is desirable for the suppression of backscatter. Because chaotic signals are non-repeating, there is also no range ambiguity.

The output of the CYDFL must be amplified and frequency doubled for underwater experimentation. Two stages of ytterbium-doped fiber amplification (YDFA) boost the CYDFL seed signal to high powers while maintaining the chaotic waveform properties. YDFAs can produce kW powers with a small physical footprint and low heat emission, with little sensitivity to vibration or ambient temperature [19]. For the chaotic transmitter, they offer an easily scalable approach to generate the high powers needed to counter absorption. Wavelength conversion from infrared to green is possible using a nonlinear second harmonic generating (SHG) crystal for frequency doubling [20]. Periodically-poled crystals can perform high efficiency SHG even of continuous-output (i.e. non-pulsed) infrared signals, with conversion efficiencies of >80% using a multi-pass resonator cavity around the crystal [21]. Each component of the chaotic lidar transmitter will be described below.

A. *Fiber Laser for Wideband, High Frequency Chaos*

The CYDFL is shown in Figure 3a. The laser's cavity resonant frequency is reduced to support multimode lasing by addition of an ultralong (100 m) passive fiber to decrease the laser mode spacing which increases the number of simultaneously lasing cavity modes [22]. This encourages mode competition and enhances the intracavity chaos, randomizing the mode phases and resulting in a noise-like signal with a non-repeating, thumbtack autocorrelation [16]. The chaotic signal is completely non-repeating, ensuring there is no range ambiguity, and the wide lasing bandwidth facilitates high resolution ranging. There is also no need for an external RF signal source or modulator, since the CYDFL generates the chaotic signal internally.

By using a fiber Braggs grating (FBG), ytterbium's many-GHz gain bandwidth can be restricted to <10 GHz lasing bandwidth. Using a 100 m passive fiber, the cavity length is extended to 120 m, for a mode spacing of 1.67 MHz; thus as many as 5400 modes may lase, all competing chaotically for the gain. This should result in a flat, uniform power spectral density (PSD) across the 0-10 GHz lasing spectrum. Designing for 90 cm of doped fiber and 225 mW available pump power at the fiber results in a calculated pump threshold of 125 mW and a lasing efficiency of 15% (Figure 3b).

B. *Fiber Amplifiers for High Power*

Two YDFAs, shown in Figure 4, are designed to amplify the 15 mW infrared signal from the YDFL to >5 W output (25 dB gain). Two stages are used to avoid the amplified spontaneous emission (ASE) associated with high gain (>23 dB) amplifier stages. A core-pumped preamplifier and a cladding-pumped

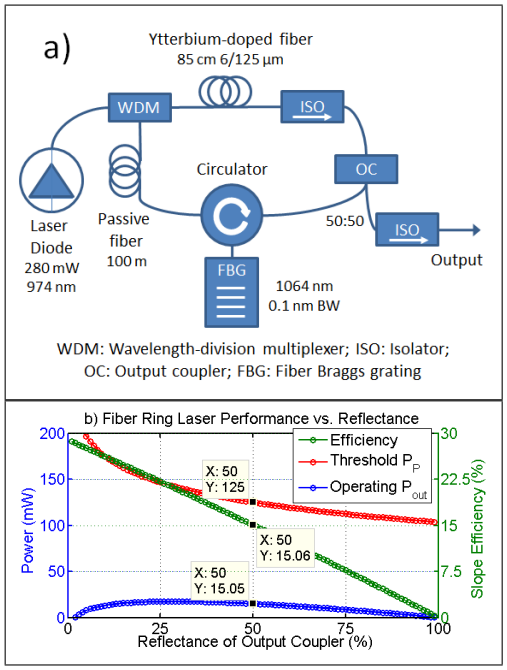

Fig. 3. Wide bandwidth, high frequency chaotic fiber laser. The novel ultralong cavity forces the simultaneous lasing of many closely spaced modes, enhancing chaos and making the output signal noise-like.

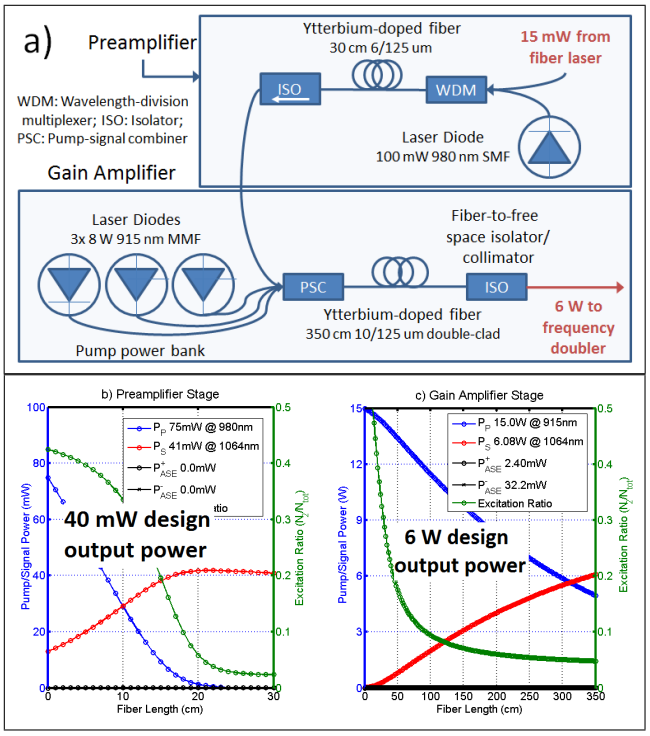

Fig. 4. Two-stage fiber amplifier chain.

gain amplifier are designed and numerically simulated. An explicit finite difference time domain (FDTD) simulation was used with a modification to the Lax-Wendroff forward-time centered-space method to efficiently solve the partial differential equations describing the bidirectional propagation of pump, signal, and ASE powers in the doped fiber [23]. These

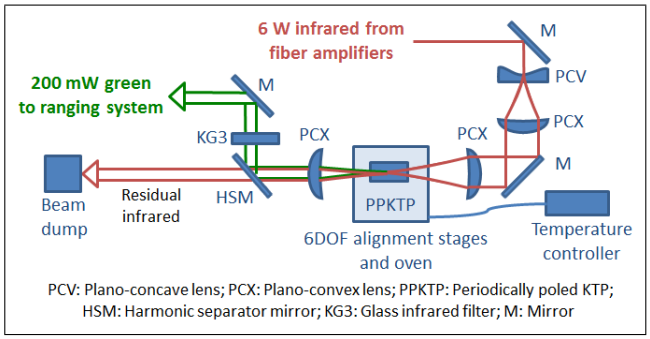

Fig. 5. Frequency doubler for conversion of infrared light to green light, as designed.

simulations yield a set of design curves. To achieve the desired overal gain and output power, the YDFAs were designed to produce 41 mW output from the preamplifier (using 75 mW pump power), and 6.1 W output from the gain amplifier (using 15 W of pump power) (Figure 4b,c).

C. Frequency Doubler for Blue-Green

The design for the frequency doubler uses a non-linear second harmonic generation crystal, and is shown in Figure 5. SHG crystals are nominally most efficient when the Rayleigh range of the focused input beam is half of the crystal length L. For the SHG used in the design, L = 20 mm, resulting in a Rayleigh range of 10 mm. Using two lenses as a telescope, the output beam from the fiber is expanded to a 2 mm beam radius. This beam is then focused by a 150 mm lens, giving a theoretical Rayleigh range of 11 mm. Based on the nominal SHG efficiency of 0.8% per 1 W input, a 4% single-pass doubling efficiency with an input of 5 W infrared 1064 nm is expected to produce a total output of 200 mW of green light at 532 nm.

III. Chaotic Lidar Transmitter Construction and Characterization

A. Ultralong Cavity Fiber Ring Laser

The constructed fiber laser is shown in Figure 6a. The laser uses a circulator ring cavity with an isolator to enforce unidirectional flow, and a 100 m long passive fiber to encourage mode competition and enhance the intracavity chaos. A 1064 nm FBG with 0.1 nm bandwidth is used for wavelength control. The ytterbium-doped fiber used is 85 cm of Liekki Yb1200-6/125DC, with a 6 μm core and a rated absorption near 250 dB/m at 976 nm pumping. The pump diode used is a fiber-coupled grating-stabilized single-mode model rated at 280 mW at 974 nm. Matching calculated predictions, lasing occurs at a threshold pump power of $\sim$125 mW delivered to the fiber, and the lasing efficiency is 15%, for an operating output power of 15 mW (with $\sim$225 mW pump delivered to the fiber). The laser operates at 1064 nm with a 10 dB optical bandwidth of 5.3 GHz, as shown in Figure 7. After opto-electronic conversion by a photodetector, the RF output signal of the fiber laser is seen to be noise-like, with a wide bandwidth extending from DC to >3 GHz

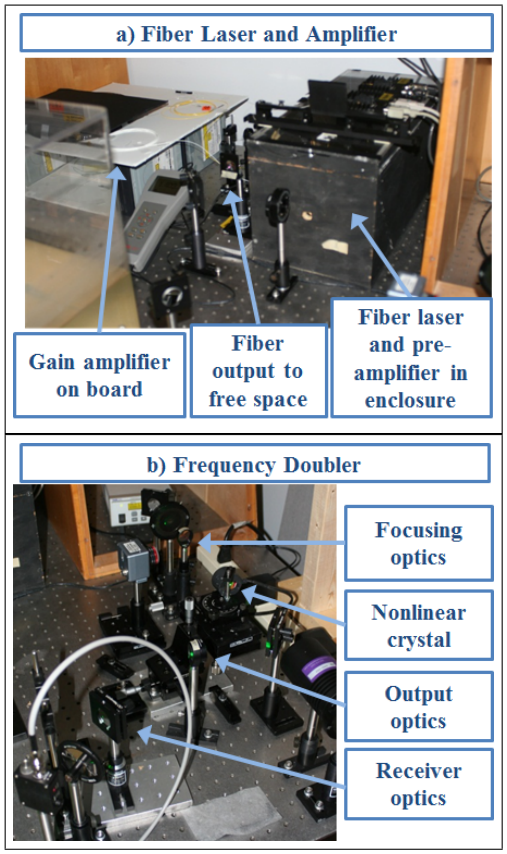

Fig. 6. 532 nm chaotic lidar transmitter experimental setup. Top: Fiber laser and two fiber amplifier stages. Bottom: Frequency doubler and associated optics.

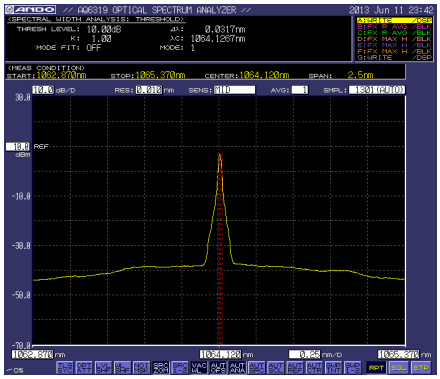

Fig. 7. Fiber laser optical spectrum. Lasing occurs at 1064 nm with a 10 dB bandwidth of 0.03 nm, or 5.3 GHz.

(see Figure 8a). The power spectral density (PSD) is flat with an associated thumbtack autocorrelation (Figure 8b,c). The nonlinear chaos of the signal can be seen by viewing either polarization individually: the single-polarization intensity trace forms a distinctive non-repeating attractor shape typical of chaotic systems (Figure 8d).

B. Two-Stage Fiber Amplifier Chain

Two fiber amplifiers boost the 15 mW 1064 nm seed signal to >6 W, as shown in Figure 9a. The first stage is a core-

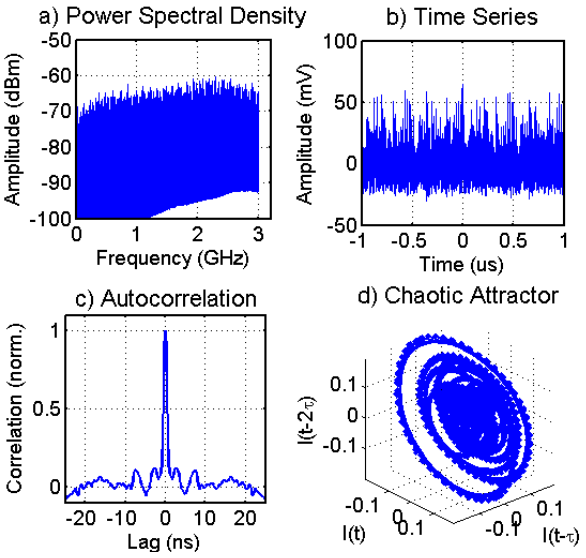

Fig. 8. Wide bandwidth, high frequency noise-like output of chaotic fiber laser. Top left: Time domain intensity modulation. Top right: Frequency domain. Bottom left: Chaotic attractor plot. Bottom right: Thumbtack autocorrelation peak has a FWHM of 1 ns (using 500 MHz receiver).

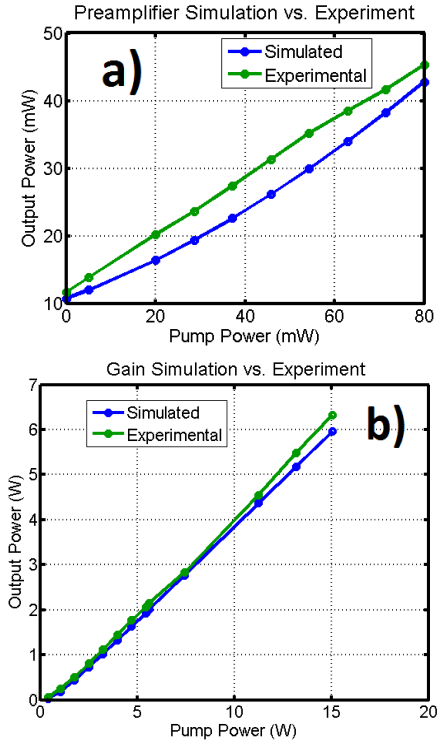

Fig. 9. Power amplification by two ytterbium-doped fiber amplifier stages. Top: Preamplifier output, experimental versus numerical simulation. Bottom: Gain amplifier output, experimental versus numerical simulation.

pumped, co-propagating YDFA using a 100 mW 980 nm single-mode pump diode with 30 cm of Yb1200-6/125DC fiber. The second stage is a cladding-pumped, co-propagating YDFA using 3 multi-mode pump diodes, each rated for 8 W at 915 nm. These diodes are each fiber-coupled to 100 μm multi-mode fiber, which is matched to a 6x1 Liekki pump-signal

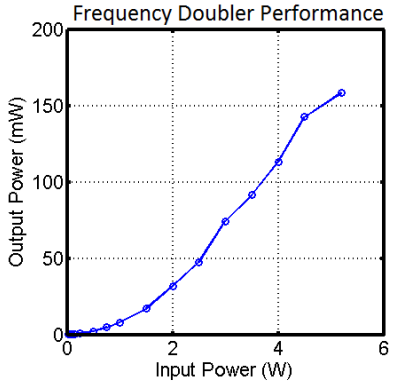

Fig. 10. Single-pass frequency doubling by a non-linear PPKTP crystal.

combiner. The combiner guides the multi-mode pump beams and the single-mode signal beam into a 10/125 μm double-clad output fiber. The output of the combiner is spliced to the doped fiber, and the splice is then recoated with a 1.38 index of refraction (n) gel to contain the pump light in the cladding. The 3.5 m doped double-clad Yb1200-10/125DC fiber has a nominal pump absorption of 1.8 dB/m at 915 nm. The output of the doped fiber is spliced to a high-power fiber-to-free-space isolator, and the splice is recoated with a n = 1.55 gel to strip any residual cladding modes out of the fiber. The isolator includes a collimating lens and outputs a 1 mm radius 1064 nm beam.

The first amplifier stage provides ~4.5 dB gain, boosting the signal to 42 mW, in good agreement with numerical simulations (Figure 9a). An optical spectrum analyzer is used to confirm that no significant ASE is generated by this stage. The second stage provides ~23.5 dB gain, amplifying the signal to 8.5 W using an estimated 15 W pump power at the fiber; here a laser line filter is used to confirm that no ASE occurs. With 1.1 dB insertion loss through the isolator and an additional 0.2 dB splice loss, 6.3 W is measured at the output of the collimator (Figure 9b).

C. Frequency Doubler

The frequency doubler and its associated optics are set up as shown in Figure 6b. A Spiricon CCD beam profiler is used to measure the Rayleigh range at ~9 mm, using a 10% threshold to define the beam waist radius. A half-wave plate is used to ensure proper polarization of the light into the crystal, as the crystal operates only on a single polarization. A temperature controller and oven enclosure maintain the crystal temperature at 72°C.

The crystal is used in a single-pass configuration. While much less efficient than a multi-pass resonator, this arrangement still produces 155 mW of green light for a 3% conversion efficiency (the incident power at the crystal is 5.2 W; the output is shown in Figure 10). A harmonic separator mirror and an ND3 KG3 glass filter are used to separate the green from the residual infrared light. A collimator lens is used to transmit the 532 nm green light out for use in the ranging system.

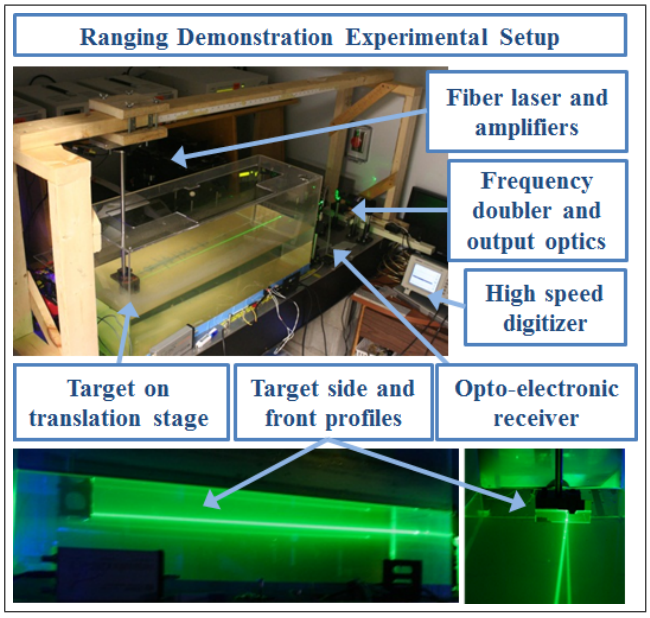

Fig. 11. Experimental setup of ranging demonstration. The target and stage allow translation 120 cm round trip.

While a single-pass configuration is used here, a multi-pass resonator (for example a bowtie cavity) could be used to improve the output conversion efficiency by more than an order of magnitude. Additional power scaling is possible simply by increasing the launched pump power into the amplifier (i.e. adding pump diodes), which could be boosted from 15 W to at least 25 W with no other change to current hardware. This would yield nonlinear improvements in the output power since the single-pass efficiency of the crystal is a quadratic function of the incident infrared power. Thus while the current output power at 532 nm is modest, it is suitable for planned experiments and it can be improved since the basic design configuration scales well to multi-watt average powers.

IV. Ranging Experiment

A. Noise Radar Receiver

Incoherent "noise radar" systems use wide bandwidth, non-repeating, noise-like or chaotic signals to achieve high resolution ranging with no ambiguous range. A noise radar receiver was designed to demonstrate underwater ranging using the chaotic transmitter, as shown in Figure 2.

From the output of frequency doubler, the green beam is split into "reference" and "return" signals using a microscope slide as a beam pickoff. 8% of the light is focused directly onto a high speed photodetector as the reference signal, and the remaining 92% is transmitted into a water tank and to the target as the return signal. This signal reflects from the target, passes back out of the tank, and is focused by a 4" collection lens onto a second photodetector. The electrical signal out of each photodetector is boosted by a low noise amplifier (LNA) and digitized by a high speed oscilloscope. The return signal line includes a DC block before the LNA to remove any unmodulated backscatter from the signal. The reference

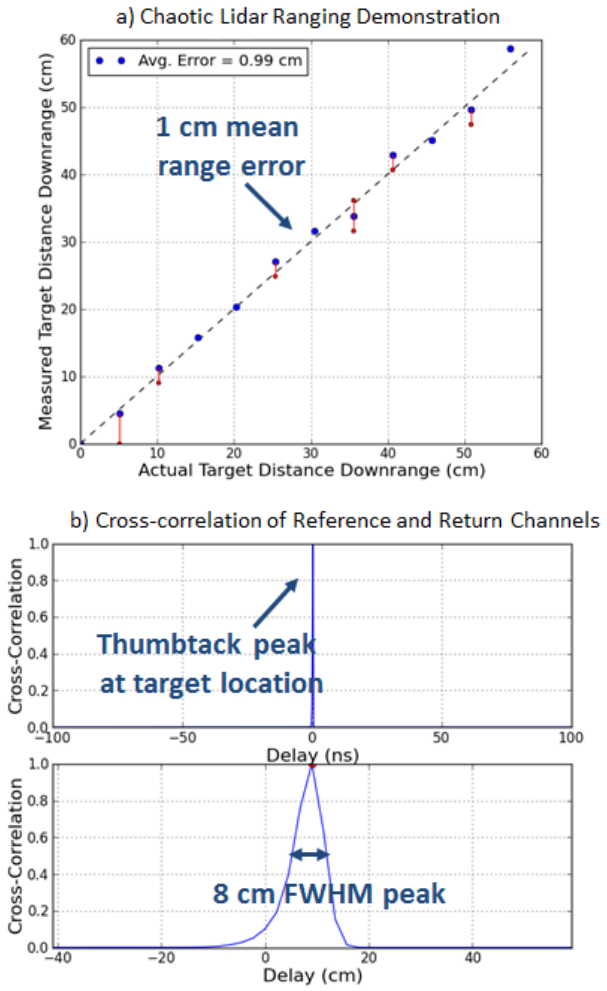

Fig. 12. Experimental results of ranging demonstration using chaotic lidar transmitter. Top: The average error is 1 cm downrange. Bottom: The range resolution as measured by FWHM peak width is ±4 cm.

and return signals are then transmitted to a PC, where they are cross-correlated, the shift between them is detected, and the range to the target is computed. The oscilloscope has a sampling rate of 5 GSPS, limiting the accuracy of the system to 0.2 ns, or 4.5 cm in water. Thus, it is expected that the cross-correlation peak center location will have an average downrange error of 0.55 cm. Further, the analog bandwidth of the digitizer is 500 MHz, so resolution of the system is theoretically receiver-limited to 2 ns. Therefore, it is expected that the cross-correlation peak width will be 45 cm corresponding to a downrange resolution of ±11.25 cm. The dwell time is receiver-limited to 2 μs. The experimental setup for the ranging demonstration is shown in Figure 11. The water tank used in the initial ranging demonstration is 100 cm long, with a front profile of 30 x 30 cm. The target used is a 10 x 5 cm plane mirror with a reflectivity above 0.95 at 532 nm. This mirror is suspended from a ±30 cm translation stage centered in the middle of the tank, allowing the target to move between 20 and 80 cm downrange. The initial ranging

demonstration is performed in clean but unfiltered water, with a measured attenuation coefficient of 0.3/m at 532 nm. Thus ranging is performed between 0.1 and 0.5 attenuation lengths round-trip.

B. Experimental Results in Water Tank

The results of the ranging demonstration are shown in Figure 12. As seen in Figure 12a, the average downrange accuracy is 1 cm, near the limit of the digitizer's sampling rate. Figure 12b shows that the cross-correlation has no periodicity: the measurement is unambiguous to at least 200 ns (45 m). The resolution as measured in correlation peak width is better than expected based on the digitizer specifications, with a 8 cm FWHM peak width and a corresponding ± 4 cm range resolution. (Presumably the digitizer's bandwidth is slightly better than specified)

V. Conclusions

We have designed and built a chaotic lidar transmitter specifically designed for the underwater environment. This transmitter operates at 532 nm with 150 mW of output power and is scalable to higher powers. The transmitter produces chaotic intensity modulation that is non-repeating to support unambiguous ranging, and wideband to support high resolution ranging and the exploration of backscatter suppression using chaotic lidar. Preliminary experimental results show 1 cm downrange accuracy and ± 4 cm downrange resolution proof-of-concept ranging in clear water.

Future work will include using the transmitter to explore the potential applications of chaotic lidar in underwater environments. Items of interest include backscatter suppression, as well as characterization of the underwater channel's temporal scattering response in a novel way that could allow channel identification and equalization, turbidity measurements, and scattering particle characterization.

VI. Acknowledgements

This work was sponsored by the Office of Naval Research under contract N00014-10-1-0906, with assistance from ASEE through the NREIP. We thank Dr. Linda Mullen, Alan Laux, and Dr. David Machewirth for their comments and suggestions.

References

[1] JS Jaffe, KD Moore, J McLean, and MP Strand. Underwater optical imaging: status and prospects. *Oceanography*, 14(3):66–76, 2001.

[2] CD Mobley. *Light and water: Radiative transfer in natural waters*, volume 592. Academic press San Diego, CA, 1994.

[3] DM Kocak, FR Dalgleish, FM Caimi, and YY Schechner. A focus on recent developments and trends in underwater imaging. *Marine Technology Society Journal*, 42(1):52–67, 2008.

[4] LJ Mullen, AJC Vieira, PR Herezfeld, and VM Contarino. Application of radar technology to aerial lidar systems for enhancement of shallow underwater target detection. *Microwave Theory and Techniques, IEEE Transactions on*, 43(9):2370–2377, 1995.

[5] LJ Mullen and VM Contarino. Hybrid lidar-radar: seeing through the scatter. *Microwave Magazine, IEEE*, 1(3):42–48, 2000.

[6] F Pellen, P Olivard, Y Guern, J Cariou, and J Lotrian. Radio frequency modulation on an optical carrier for target detection enhancement in sea-water. *Journal of Physics D: Applied Physics*, 34(7):1122, 2001.

[7] B Cochenour, L Mullen, and J Muth. Modulated pulse laser with pseudorandom coding capabilities for underwater ranging, detection, and imaging. *Applied Optics*, 50(33):6168–6178, 2011.

[8] F Pellen, V Jezequel, G Zion, and BL Jeune. Detection of an underwater target through modulated lidar experiments at grazing incidence in a deep wave basin. *Applied optics*, 51(31):7690–7700, 2012.

[9] P Perez, WD Jemison, L Mullen, and A Laux. Techniques to enhance the performance of hybrid lidar-radar ranging systems. In *Oceans, 2012*, pages 1–6. IEEE, 2012.

[10] D Illig, WD Jemison, L Rumbaugh, R Lee, A Laux, and L Mullen. Technique to extend unambiguous range of hybrid lidar-radar systems. In *OCEANS 2013, MTS/IEEE San Diego*, Sept. 2013.

[11] F Pellen, X Intes, P Olivard, Y Guern, J Cariou, and J Lotrian. Determination of sea-water cut-off frequency by backscattering transfer function measurement. *Journal of Physics D: Applied Physics*, 33(4):349, 2000.

[12] L Mullen, A Laux, and B Cochenour. Propagation of modulated light in water: implications for imaging and communications systems. *Applied optics*, 48(14):2607–2612, 2009.

[13] RM Narayanan, Y Xu, PD Hoffmeyer, and JO Curtis. Design, performance, and applications of a coherent ultra-wideband random noise radar. *Optical Engineering*, 37(6):1855–1869, 1998.

[14] FY Lin and JM Liu. Chaotic lidar. *Selected Topics in Quantum Electronics, IEEE Journal of*, 10(5):991–997, 2004.

[15] Y Wang, B Wang, and A Wang. Chaotic correlation optical time domain reflectometer utilizing laser diode. *Photonics Technology Letters, IEEE*, 20(19):1636–1638, 2008.

[16] LK Rumbaugh, WD Jemison, Y Li, and TA Wey. Wide bandwidth source for high resolution ranging. In *Ultra-Wideband (ICUWB), 2012 IEEE International Conference on*, pages 482–485. IEEE, 2012.

[17] P-H Chen, MC Shastry, C-P Lai, and RM Narayanan. A portable real-time digital noise radar system for through-the-wall imaging. *Geoscience and Remote Sensing, IEEE Transactions on*, 50(10):4123–4134, 2012.

[18] QL Williams, J Garcia-Ojalvo, and R Roy. Fast intracavity polarization dynamics of an erbium-doped fiber ring laser: Inclusion of stochastic effects. *Physical Review A*, 55(3):2376, 1997.

[19] DJ Richardson, J Nilsson, and WA Clarkson. High power fiber lasers: current status and future perspectives [invited]. *J. Opt. Soc. Am. B*, 27(11):B63–B92, Nov 2010.

[20] F Hanson and S Radic. High bandwidth underwater optical communication. *Appl. Opt.*, 47(2):277–283, Jan 2008.

[21] ZY Ou, SF Pereira, ES Polzik, and HJ Kimble. 85% efficiency for cw frequency doubling from 1.08 to 0.54, μm. *Optics letters*, 17(9):640–642, 1992.

[22] V Roy, M Piche, F Babin, and G Schinn. Nonlinear wave mixing in a multilongitudinal-mode erbium-doped fiber laser. *Optics express*, 13(18):6791–6797, 2005.

[23] Y Wang and H Po. Dynamic characteristics of double-clad fiber amplifiers for high-power pulse amplification. *Lightwave Technology, Journal of*, 21(10):2262–2270, 2003.